Journal of Zhejiang University SCIENCE A
ISSN 1673-565X (Print); ISSN 1862-1775 (Online)
www.zju.edu.cn/jzus; www.springerlink.com
E-mail: jzus@zju.edu.cn

3D wind-induced response analysis of a cable-membrane structure*

Jun-jie LUO, Da-jian HAN

(*State Key Laboratory of Subtropical Architecture Science, School of Civil Engineering and Transportation, South China University of Technology, Guangzhou 510640, China*)

E-mail: axljj@163.com; ardjhan@scut.edu.cn

Received June 9, 2008; Revision accepted Aug. 31, 2008; Crosschecked Dec. 29, 2008

Abstract: Wind loading is a dominant factor for design of a cable-membrane structure. Three orthogonal turbulent components, including the longitudinal, lateral and vertical wind velocities, should be taken into account for the wind loads. In this study, a stochastic 3D coupling wind field model is derived by the spectral representation theory. The coherence functions of the three orthogonal turbulent components are considered in this model. Then the model is applied to generate the three correlated wind turbulent components. After that, formulae are proposed to transform the velocities into wind loads, and to introduce the modified wind pressure force. Finally, a wind-induced time-history response analysis is conducted for a 3D cable-membrane structure. Analytical results indicate that responses induced by the proposed wind load model are 10%~25% larger than those by the conventional uncorrelated model, and that the responses are not quite influenced by the modified wind pressure force. Therefore, we concluded that, in the time-history response analysis, the coherences of the three orthogonal turbulent components are necessary for a 3D cable-membrane structure, but the modified wind pressure force can be ignored.

Key words: Cable-membrane structures, Time-history analysis, Coherence, Gust response factor
doi:10.1631/jzus.A0820430 **Document code:** A **CLC number:** TU318; TU393.3; TU311.3

INTRODUCTION

Wind loading response analysis is generally needed for design of a 3D large-span structure. Aerodynamic mechanisms of low-rise building roofs under the wind internal and external loading in frequency domain have been investigated by Yu *et al*.(2006; 2008). However, as for a large-span 3D cable-membrane spatial roof structure, the wind-excited dynamic response in frequency domain is no more suitable owing to its nonlinearity. At this time, time-history analysis is a proper alternative (Shen, 2006). Hence, it is necessary to simulate the time-history of the wind load properly.

Stochastic wind loads can be obtained from wind velocities based on the quasi-steady theory. For a cable-membrane roof structure, three orthogonal turbulent components, including longitudinal, lateral and vertical wind velocities, are necessary to be considered. In conventional methods, the three wind velocities are generated separately and then transformed into wind loads (Li *et al*., 2004). Thus, the three wind components are assumed uncorrelated. However, experimental measurements show that the three stochastic wind turbulent components are correlated (Panofsky and Dutton, 1984), especially between the longitudinal component and the vertical component. Therefore, in the 3D wind-induced dynamic response analysis, it needs to investigate the correlations among the three wind turbulent components.

In this study, a stochastic 3D correlated wind velocity field model is proposed based on the spectral representation theory. Then, formulae for transforming stochastic wind velocities into wind loads are derived in detail. And the modified wind pressure force is also introduced. Finally, the wind loads are applied to perform a time-history response analysis for a spatial 3D cable-membrane structure. The

* Project (No. 2004Z3-E0351) supported by the Guangzhou Scientific and Technological Research Project, China

results obtained by the proposed model are compared with those done by the conventional methods and some valuable conclusions are drawn.

DERIVATION OF THE 3D STOCHASTIC WIND FIELD MODEL

Consider a 3D wind field with n spatial nodes, the mean wind velocity of Node j can be defined as the logarithmic profile (Simiu and Scanlan, 1986) of

$$\overline{u}_j = 2.5u_* \ln(z_j / z_0), \tag{1}$$

where z_j is the height of Node j; z_0 is the roughness length, and u_* is the surface friction velocity. The 3D stochastic wind velocity time-history vector of Node j is a zero-mean Gaussian stationary process, expressed as

$$\boldsymbol{u}_j(t) = \{u_j(t),\ v_j(t),\ w_j(t)\}^{\mathrm{T}},\ j = 1, 2, ..., n, \tag{2}$$

where $u_j(t)$, $v_j(t)$, $w_j(t)$ are the longitudinal, lateral, and vertical wind velocities of Node j corresponding to x, y, z directions, respectively. In the following, for simplicity, the suffix j is omitted. Assume that $\boldsymbol{S}$ is a corresponding complex-valued cross-power spectral density function (CPSDF) matrix of the process. Many observations have proven that $v(t)$ is uncorrelated with $u(t)$ and $w(t)$ (Panofsky and Dutton, 1984). Hence, $\boldsymbol{S}$ can be expressed as

$$\boldsymbol{S}(\omega) = \begin{bmatrix} \boldsymbol{S}^1(\omega) & \boldsymbol{0} \\ \boldsymbol{0} & \boldsymbol{S}^2(\omega) \end{bmatrix}, \tag{3}$$

where $\boldsymbol{S}^1(\omega)$ is a sub-matrix considering the correlation of $u(t)$ and $w(t)$. The element in $\boldsymbol{S}^1(\omega)$ is expressed as

$$\boldsymbol{S}^1_{jk}(\omega) = \begin{bmatrix} S^{uu}_{jk}(\omega) & S^{uw}_{jk}(\omega) \\ S^{wu}_{jk}(\omega) & S^{ww}_{jk}(\omega) \end{bmatrix}. \tag{4}$$

$\boldsymbol{S}^2(\omega)$ is the other sub-matrix, where the element is expressed as

$$S^2_{jk}(\omega) = S^{vv}_{jk}(\omega). \tag{5}$$

As can be seen in Eqs.(4) and (5), there are two types of elements in the sub-matrices. One is the type of diagonal elements with real-values and named as self-power spectral density functions (SPSDFs) (α=u, v, w); the other is the type of off-diagonal complex-valued elements (α, β=u, v, w; $j \neq k$) defined as

$$S^{\alpha\beta}_{jk}(\omega) = \sqrt{S^{\alpha\alpha}_{jj}(\omega) S^{\beta\beta}_{kk}(\omega)}\, Coh^{\alpha\beta}_{jk}(\omega) \exp[\mathrm{i}\theta_{jk}(\omega)], \tag{6}$$

where $Coh^{\alpha\beta}_{jk}(\omega)$ is the coherence function, $\theta_{jk}(\omega)$ the phase angle and $\mathrm{i} = \sqrt{-1}$.

In Eq.(3), a 3D stochastic wind field can be divided into a 2D wind field of the components u and w as well as a 1D wind field of v. The 2D stochastic wind field model is derived in the following.

Decomposing $\boldsymbol{S}^1(\omega)$ by the Cholesky factorization, a lower triangle matrix $\boldsymbol{H}(\omega)$ is obtained as

$$\boldsymbol{H}(\omega)\boldsymbol{H}^{*\mathrm{T}}(\omega) = \boldsymbol{S}^1(\omega), \tag{7}$$

where "*" denotes the complex conjugate of $\boldsymbol{H}(\omega)$. The properties of the elements in $\boldsymbol{H}(\omega)$ are

$$\begin{aligned} &H^{\eta\mu}_{jj}(\omega) = H^{\eta\mu}_{jj}(-\omega) \quad (\eta, \mu = u, w), \\ &H^{\eta\mu}_{jk}(\omega) = (H^{\eta\mu}_{jk})^*(-\omega) \quad (j > k), \\ &H^{\eta\mu}_{jk}(\omega) = \left|H^{\eta\mu}_{jk}(\omega)\right| \exp[\mathrm{i}\,\theta_{jk}(\omega)], \end{aligned} \tag{8}$$

where $\theta_{jk}(\omega)$ is given by

$$\theta_{jk}(\omega) = \arctan\left\{\frac{\mathrm{Im}\left[H^{\eta\mu}_{jk}(\omega)\right]}{\mathrm{Re}\left[H^{\eta\mu}_{jk}(\omega)\right]}\right\}. \tag{9}$$

It is an odd function of ω, so that

$$\theta_{jk}(\omega) = -\theta_{jk}(-\omega). \tag{10}$$

Actually, $\theta_{jk}(\omega)$ represents time lag of the mean wind arriving at two spatial points. According to the Taylor's frozen assumption (Panofsky and Dutton, 1984), $\theta_{jk}(\omega)$ is expressed as

$$\theta_{jk}(\omega)=\omega\frac{(x_j-x_k)}{[\overline{u}_j+\overline{u}_k]/2}. \tag{11}$$

Hence, the stochastic 2D wind velocity vector $\boldsymbol{f}^1(t)=\{u_1(t), w_1(t), \cdots, u_n(t), w_n(t)\}^{\mathrm{T}}$ can be expressed by the spectral representation theory as

$$\boldsymbol{f}^1(t)=\mathrm{Re}[\int_0^{+\infty}\exp(\mathrm{i}\omega t)\mathrm{d}\boldsymbol{Z}(\omega)],\ \omega>0, t>0, \tag{12}$$

where $\mathrm{d}\boldsymbol{Z}(\omega)$ is a complex-valued stochastic process matrix with the following three conditions:

$$\text{(i) } E[\mathrm{d}\boldsymbol{Z}(\omega)]=\boldsymbol{0}, \tag{13}$$

$$\text{(ii) } E[\mathrm{d}\boldsymbol{Z}(\omega)\mathrm{d}\boldsymbol{Z}^*(\omega)]=E[|\mathrm{d}\boldsymbol{Z}(\omega)|^2]=2\boldsymbol{S}^1(\omega)\mathrm{d}\omega, \tag{14}$$

$$\text{(iii) } E[\mathrm{d}\boldsymbol{Z}(\omega)\mathrm{d}\boldsymbol{Z}^*(\overline{\omega})]=\boldsymbol{0},\ \overline{\omega}>0,\ \text{and}\ \omega\neq\overline{\omega}, \tag{15}$$

where $E[\cdot]$ denotes the statistical mean value operator. Therefore, $\mathrm{d}\boldsymbol{Z}(\omega)$ can be assumed as

$$\mathrm{d}\boldsymbol{Z}(\omega)=\sqrt{2\mathrm{d}\omega}\,\boldsymbol{H}(\omega)\boldsymbol{T}(\omega), \tag{16}$$

where the vector $\boldsymbol{T}(\omega)=\{\exp[\mathrm{i}\phi_1(\omega)], \exp[\mathrm{i}\phi_2(\omega)], \cdots, \exp[\mathrm{i}\phi_{2n-1}(\omega)], \exp[\mathrm{i}\phi_{2n}(\omega)]\}^{\mathrm{T}}$, and $\phi_p(\omega)$ (p=1, 2, ⋯, 2n) are the random phase angles distributed uniformly over the interval [0,2π]. Substituting Eq.(16) into Eqs.(13)~(15) and applying Eqs.(8) and (10), it is easy to verify that Eq.(16) can satisfy the three conditions. Therefore, substituting Eq.(16) into Eq.(12), the vector $\boldsymbol{f}^1(t)$ is then represented as

$$\begin{aligned}\boldsymbol{f}^1(t)&=\mathrm{Re}[\int_0^{+\infty}\sqrt{2\mathrm{d}\omega}\,\boldsymbol{H}(\omega)\boldsymbol{W}(\omega)]\\&\approx\mathrm{Re}[\sqrt{2\Delta\omega}\sum_{l=1}^{N}\boldsymbol{H}(\omega_l)\boldsymbol{W}(\omega_l)],\end{aligned} \tag{17}$$

where the vector $\boldsymbol{W}(\omega_l)=\{\exp[\mathrm{i}(\phi_1+\omega_l t)], \exp[\mathrm{i}(\phi_2+\omega_l t)], \cdots, \exp[\mathrm{i}(\phi_{2n-1}+\omega_l t)], \exp[\mathrm{i}(\phi_{2n}+\omega_l t)]\}^{\mathrm{T}}$. Assume that the radian frequency range is $[\omega_{\min}, \omega_{\max}]$ and that N is a large enough positive integer. Then the discrete frequency points are $\omega_l=\omega_{\min}+(l-1/2)\Delta\omega$ (l=1, 2, ⋯, N) with increment of $\Delta\omega=(\omega_{\max}-\omega_{\min})/N$.

As for the wind velocity vector $\boldsymbol{f}^2(t)=\{v_1(t), v_2(t), \cdots, v_n(t)\}^{\mathrm{T}}$, it is just a simplification of the 2D model and not to be listed here. Details can be found in (Deodatis, 1996).

DESCRIPTION OF THE WIND LOADS AND THE NONLINEAR DYNAMIC EQUATION OF THE STRUCTURE

Stochastic wind velocity time-histories can be transformed into wind load time-histories based on the quasi-steady theory (Uematsu and Isyumov, 1999). Considering a 3D wind loading field, the wind loads acting on Node j can be defined as

$$F_j(t)=0.5\rho|\boldsymbol{V}(t)|^2 C_{\mathrm{p}}[\theta(t),\beta(t)]A, \tag{18}$$

where ρ is the air density and A the area of Node j subjected to wind loads. The vector $\boldsymbol{V}(t)$ is the transient wind velocity of Node j. $C_{\mathrm{p}}[\theta(t),\beta(t)]$ is the wind pressure coefficient while $\theta(t)$ and $\beta(t)$ are the transient horizontal and vertical wind angles, respectively.

The components of $\boldsymbol{V}(t)$ are indicated in Fig.1, where $\overline{u}$, $\overline{v}$, and $\overline{w}$ denote the longitudinal, lateral and vertical mean wind velocities, respectively, and $u_{\mathrm{s}}(t)$, $v_{\mathrm{s}}(t)$, $w_{\mathrm{s}}(t)$ are the transient vibration velocities of Node j in x, y and z directions, respectively. Then, $|\boldsymbol{V}(t)|^2$ can be expressed as

$$\begin{aligned}|\boldsymbol{V}(t)|^2&=[\overline{u}+u(t)-u_{\mathrm{s}}(t)]^2+[\overline{v}+v(t)-v_{\mathrm{s}}(t)]^2\\&\quad+[\overline{w}+w(t)-w_{\mathrm{s}}(t)]^2\\&=\overline{u}^2+2\overline{u}[u(t)-u_{\mathrm{s}}(t)]+[u(t)-u_{\mathrm{s}}(t)]^2\\&\quad+\overline{v}^2+2\overline{v}[v(t)-v_{\mathrm{s}}(t)]+[v(t)-v_{\mathrm{s}}(t)]^2\\&\quad+\overline{w}^2+2\overline{w}[w(t)-w_{\mathrm{s}}(t)]+[w(t)-w_{\mathrm{s}}(t)]^2.\end{aligned} \tag{19}$$

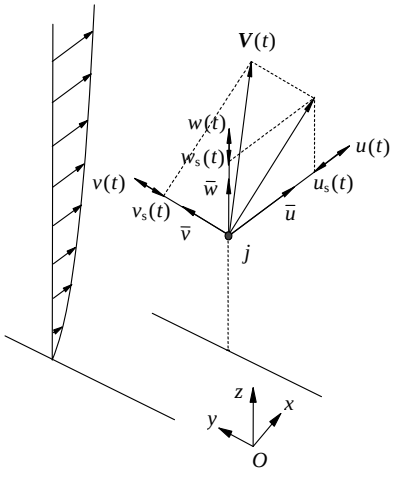

Fig.1 Wind velocity components of Node *j*

Now, some simplifications are made in Eq.(19). Firstly, observations (Shiau and Chen, 2002) show that $u(t)$, $v(t)$, $w(t)$ and $u_s(t)$, $v_s(t)$, $w_s(t)$ can be neglected compared to the magnitude of $\bar{u}$. Hence, $[u(t)-u_s(t)]^2$, $[v(t)-v_s(t)]^2$ and $[w(t)-w_s(t)]^2$ are ignored. Secondly, observations also indicate that no matter what kind of terrain the wind blows over, $\bar{w}$ is correlated with $\bar{u}$. The relationship between them is $\bar{w}=\bar{u}\tan\alpha$ ($|\alpha|\leq 10°$) (Yang and Sun, 1997). Therefore, the maximum value of $\bar{w}$ adopted for the response of the structure is $0.18\bar{u}$. With this condition, $\bar{w}^2=0.0324\bar{u}^2$ and $2\bar{w}[w(t)-w_s(t)]\ll\bar{u}$, so the two terms are also ignored. Finally, $\bar{v}$ equals to zero (Panofsky and Dutton, 1984), thus $\bar{v}^2$ and $2\bar{v}[v(t)-v_s(t)]$ are zero. Now Eq.(19) is rewritten as

$$|\boldsymbol{V}(t)|^2=\bar{u}^2+2\bar{u}[u(t)-u_s(t)]. \tag{20}$$

In the linearized quasi-steady vector model, $C_p[\theta(t),\beta(t)]$ is approximated by a Taylor polynomial of the first-order as

$$\begin{aligned}C_p[\theta(t),\beta(t)]&=C_p[\theta_0,\beta_0]\\&+[\theta(t)-\theta_0]\frac{\partial C_p[\theta(t),\beta(t)]}{\partial\theta}\bigg|_{\substack{\theta=\theta_0\\\beta=\beta_0}}\\&+[\beta(t)-\beta_0]\frac{\partial C_p[\theta(t),\beta(t)]}{\partial\beta}\bigg|_{\substack{\theta=\theta_0\\\beta=\beta_0}},\end{aligned} \tag{21}$$

where θ_0, β_0 are the mean wind angles in horizontal and vertical directions, respectively. $\theta(t)$ is the transient horizontal wind angle, while $\beta(t)$ is the transient vertical one. Two terms in Eq.(21) can be expressed as

$$\begin{aligned}\theta(t)-\theta_0&=\frac{v(t)-v_s(t)}{\bar{u}},\\\beta(t)-\beta_0&=\frac{\bar{w}+w(t)-w_s(t)}{\bar{u}}.\end{aligned} \tag{22}$$

Let

$$C_{pu}=C_p[\theta_0,\beta_0],\quad C_{pv}=\frac{\partial C_p[\theta(t),\beta(t)]}{\partial\theta}\bigg|_{\substack{\theta=\theta_0\\\beta=\beta_0}},$$

$$C_{pw}=\frac{\partial C_p[\theta(t),\beta(t)]}{\partial\beta}\bigg|_{\substack{\theta=\theta_0\\\beta=\beta_0}} \tag{23}$$

be the shape coefficients of the wind loads induced by the longitudinal, lateral and vertical wind velocities, respectively. In practical application, C_{pu} is obtained by wind tunnel test or by real measurement. However, C_{pv} is hard to be measured, so it is approximately expressed as

$$C_{pv}=\frac{\partial C_p[\theta(t),\beta(t)]}{\partial\theta}\bigg|_{\substack{\theta=\theta_0\\\beta=\beta_0}}\approx\frac{C_{pu}^k-C_{pu}}{\theta_k-\theta_0}, \tag{24}$$

where $C_{pu}^k-C_{pu}$ is the difference of the shape coefficient as the longitudinal angle changing from θ_0 to θ_k. The empirical value of C_{pw} is over the range of [−0.5, −0.3] (Shen *et al.*, 2006). So the most disadvantageous value of −0.5 is taken to obtain the maximum response of the structure. Finally, combining Eqs.(20) to (24), Eq.(18) can be expressed as

$$\begin{aligned}F_j(t)&=0.5\rho A\{\bar{u}^2+2\bar{u}[u(t)-u_s(t)]\}\\&\times\left[C_{pu}+\frac{v(t)-v_s(t)}{\bar{u}}C_{pv}+\frac{\bar{w}+w(t)-w_s(t)}{\bar{u}}C_{pw}\right]\\&\approx 0.5\rho A\bar{u}[C_{pu}\bar{u}+0.18C_{pw}\bar{u}]\\&+0.5\rho A\bar{u}[2C_{pu}u(t)+C_{pv}v(t)+C_{pw}w(t)]\\&-0.5\rho A\bar{u}[2C_{pu}u_s(t)+C_{pv}v_s(t)+C_{pw}w_s(t)]\\&=F_m+F_t(t)-F_d(t),\end{aligned} \tag{25}$$

where terms without $\bar{u}$ are omitted for the same reason mentioned for Eq.(20). F_m and $F_t(t)$ are the wind forces caused by the mean wind velocities and the turbulent wind velocities, respectively. $F_d(t)$ can be viewed as the modified wind pressure force induced by the vibration velocity of the node. Then, the equation of motion is obtained as

$$\boldsymbol{M}\ddot{\boldsymbol{x}}(t)+(\boldsymbol{C}+\boldsymbol{C}_a)\dot{\boldsymbol{x}}(t)+\boldsymbol{K}\boldsymbol{x}(t)=\boldsymbol{F}_m+\boldsymbol{F}_t(t), \tag{26}$$

where $\boldsymbol{M}$, $\boldsymbol{K}$, $\boldsymbol{C}$, and $\boldsymbol{C}_a$ are the lumped mass matrix, the stiffness matrix, the structural damping matrix, and the modified wind pressure force matrix, respectively. $\boldsymbol{F}_m$ is the mean wind loading vector and $\boldsymbol{F}_t(t)$ the turbulent wind loading vector. $\boldsymbol{x}(t)$, $\dot{\boldsymbol{x}}(t)$, $\ddot{\boldsymbol{x}}(t)$ are the displacement, velocity and acceleration vectors, respectively.

DYNAMIC RESPONSE ANALYSIS OF THE STRUCTURE

A dynamic response time-history analysis under the 3D wind loads is performed for a simple cable-membrane structure. It is a square saddle roof composed of four side cables and membrane. Its four corners are fixed by supports. The diagonal length L of the structure is 10 m. And the difference between high position and low position is h =0.825 m. The sectional area of the cable is 0.0002 m^2 with a pretension force of 45 kN. The thickness of the membrane is 0.001 m with the pretension stress of 2 MPa. The FEM model of the structure is demonstrated in Fig.2. The shape coefficients for the wind loads under six longitudinal wind azimuths are shown in Fig.3 (Yang and Shen, 1996).

Parameters for wind velocity field simulation are given below.

(1) Self-power spectral density functions

The one-sided SPSDFs $S_{jj}^{\alpha\alpha}(\omega)\,(\alpha=u,v,w)$ advised by the Engineering Sciences Data Unit (ESDU85020, 1985) are adopted as follows:

$$S_{jj}^{uu}(\omega)=\frac{1}{2\pi}\frac{4\sigma_u^2 L_u/\overline{u}_j}{\left\{1+70.8\left[\omega L_u/(2\pi\overline{u}_j)\right]^2\right\}^{5/6}}, \tag{27}$$

$$S_{jj}^{\varepsilon\varepsilon}(\omega)=\frac{1}{2\pi}\frac{4(\sigma_\varepsilon^2 L_\varepsilon/\overline{u}_j)\left\{1+755.2\left[\omega L_\varepsilon/(2\pi\overline{u}_j)\right]^2\right\}}{\left\{1+283.2\left[\omega L_\varepsilon/(2\pi\overline{u}_j)\right]^2\right\}^{11/6}}, \tag{28}$$

$\varepsilon=v,\ w,$

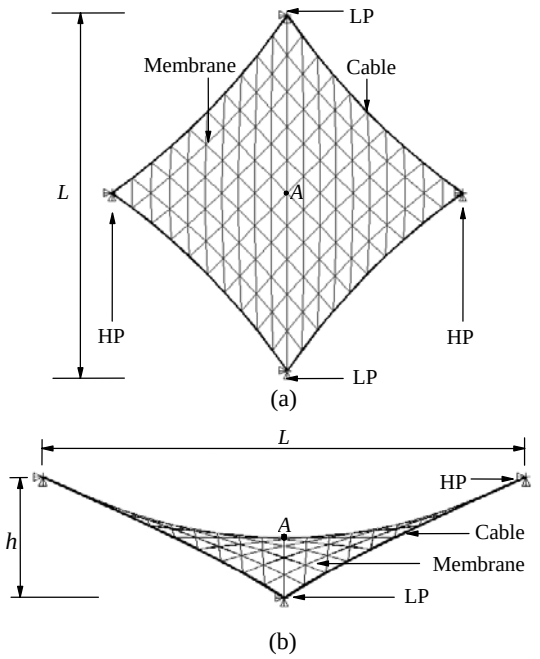

Fig.2 FEM model of the structure. (a) Top view; (b) Front view. HP: high position; LP: low position

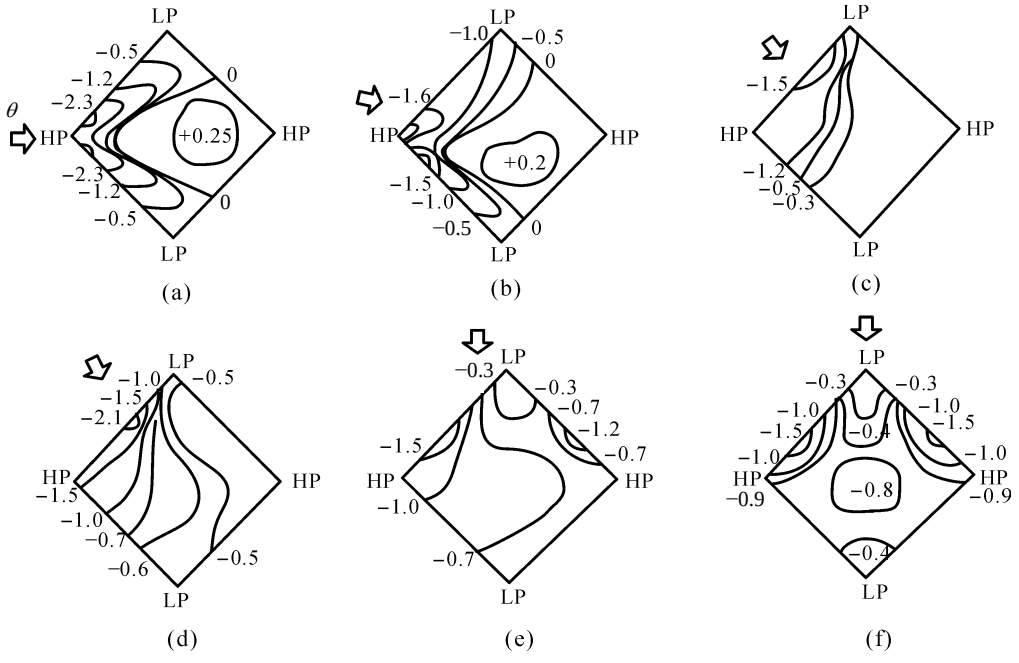

Fig.3 Shape coefficients of the wind loads under six longitudinal wind azimuths θ. (a) θ=0°; (b) θ=15°; (c) θ=45°; (d) θ=60°; (e) θ=75°; (f) θ=90°. HP: high position; LP: low position

where σ_α^2 is the variance of the turbulent velocity of component α and defined as

$$\sigma_\alpha^2 = \gamma_\alpha (u_*)^2, \tag{29}$$

where γ_α is named as the turbulence intensity factor. Empirical formulae for γ_α of three wind directions developed by Solari and Piccardo (2001) are

$$\begin{aligned} &\gamma_u = 6 - 1.1 \arctan[\ln z_0 + 1.75], \\ &\gamma_v = 0.55\gamma_u, \quad \gamma_w = 0.25\gamma_u, \end{aligned} \tag{30}$$

where L_α is the integral length scale of turbulent and expressed as

$$L_u = 300(z_j / 200)^{0.67+0.05\ln z_0}, L_v = 0.25L_u, L_w = 0.1L_u. \tag{31}$$

According to the design code (GB50009-2001, 2002), we assume that the structure is on the location of Type B, thereby the two important parameters are taken as z_0=0.02 m, u_*=1.82 m/s.

(2) Three types of coherence functions (COHFs)

1) The spatial COHF $Coh_{jk}^{\alpha\alpha}(\omega)$ represents the correlation of Nodes j and k in the same wind direction (Simiu and Scanlan, 1986)

$$Coh_{jk}^{\alpha\alpha}(\omega) = \exp\left\{-\frac{\omega\sqrt{\sum_r C_{r\alpha}^2 |r_j - r_k|^2}}{\pi[\bar{u}_j + \bar{u}_k]}\right\}, \tag{32}$$
$$j \neq k,\ r_j = x_j, y_j, z_j,\ r_k = x_k, y_k, z_k,$$

where C_{xu}=3.0, C_{xv}=3.0, C_{xw}=0.5, C_{yu}=10.0, C_{yv}=6.5, C_{yw}=6.5, C_{zu}=10.0, C_{zv}=6.5, C_{zw}=3.0.

2) The point COHF $Coh_{jj}^{uw}(\omega)$ describes the relationships of turbulent components u and w at Node j. It can be written as (Solari and Piccardo, 2001)

$$Coh_{jj}^{uw}(\omega) = -\frac{1}{\kappa_{uw}} \frac{1}{\sqrt{1 + 0.4[\omega L_u / (2\pi\bar{u}_j)]}}, \tag{33}$$

where κ_{uw} termed the point coherence scaling factor and

$$\kappa_{uw} = \frac{B_{uw}\sigma_u(z_j)\sigma_w(z_j)}{(u_*)^2}, \quad B_{uw} = 1.11\left(\frac{L_w}{L_u}\right)^{0.21}. \tag{34}$$

3) The spatial and point COHF $Coh_{jk}^{uw}(\omega)$ represents the relationship of Node j and Node k between turbulent components u and w. It is defined as (Solari and Piccardo, 2001)

$$\begin{aligned} Coh_{jk}^{uw}(\omega) = &-\sqrt{Coh_{jj}^{uw}(\omega)\, Coh_{kk}^{uw}(\omega)} \\ &\times \sqrt{Coh_{jk}^{uu}(\omega)\, Coh_{jk}^{ww}(\omega)}. \end{aligned} \tag{35}$$

The 3D stochastic wind velocity field with 200 spatial nodes is generated. To improve computational efficiency, a method provided by Luo and Han (2008) is used in computation. The simulation time is 204.8 s. The time interval Δt is 0.025 s. A comparison of the target self-correlation functions and the self-correlation functions of the simulated samples is shown in Fig.4. It can be seen that the simulation results coincide with the target ones well. Therefore, the wind loads generated by the proposed method is applicable to wind response analysis of the structure.

Now, the time-history response analyses under different wind azimuths are conducted by the commercial software ANSYS. There are five loadcases taken into account: (A) Only a longitudinal wind load without considering the modified wind pressure force; (B) The uncorrelated longitudinal and vertical wind loads without the modified wind pressure force; (C) The uncorrelated longitudinal, lateral and vertical wind loads without the modified wind pressure force; (D) The correlated longitudinal, lateral and vertical wind loads without the modified wind pressure force; (E) The correlated longitudinal, lateral and vertical wind loads with the modified wind pressure force.

In computation, the modified wind pressure

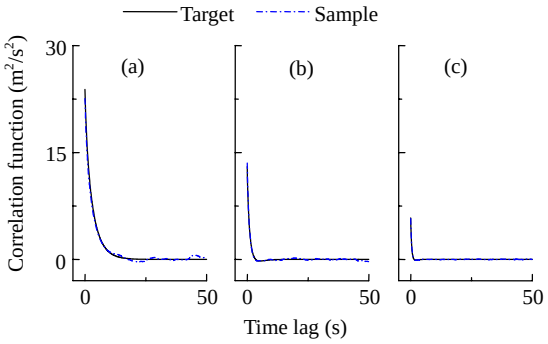

Fig.4 Verifications of the self-correlation functions of Node *A*. (a) *u*; (b) *v*; (c) *w*

force is described by the Matrix 27 element of the software. In addition, it should be mentioned that the SPSDFs and corresponding parameters are also applied to generate the three uncorrelated wind loads for comparisons with the correlated loads cases.

Five types of response are considered: (a) stress of the cable; (b) stress of the membrane; (c) nodal displacement *x*; (d) nodal displacement *y*; (e) nodal displacement *z*. Since the traditional gust loading factor is no more available for the case of the structural nonlinearity, the gust response factor (GRF) is adopted and given by (Shen *et al.*, 2006)

$$\beta_j^k = 1 + \frac{\lambda \sigma_j^k}{|m_j^k|}, \tag{36}$$

where β_j^k is the GRF for the *j*th element of the *k*th type of the response; σ_j^k, m_j^k are the standard deviation and the mean value, respectively. λ is the peak value factor and equals 3.5. Note that a small value of m_j^k will lead to an unreasonable value for β_j^k. Actually, the maximum value of the response is a determinate factor for design. Thus, instead of Eq.(36), the GRF of the *k*th type of response is applied (Chen *et al.*, 2005) as

$$\beta^k = \frac{\{|\beta_j^k m_j^k|\}_{\max}}{\{|m_j^k|\}_{\max}}, \tag{37}$$

where $\{|\beta_j^k m_j^k|\}_{\max}$ is the maximum absolute value of the *k*th type of the response. In this way, the GRFs for the response are shown in Figs.5(a)~5(e). It can be seen from the results that

(1) The values of β^k are close to each other for Loadcases (A), (B), and (C). That means there are no obvious differences of the responses while the three uncorrelated wind loads are applied to the structure.

(2) The results of Loadcase (D) are nearly the same as those of Loadcase (E). Hence, the modified wind pressure force has little influence on the dynamic response. The reason is that vibration velocity of the structure changes so slowly that the force is not large;

(3) The maximum stress GRFs of the cable and the membrane for Loadcase (D) are both 2.5, while those for Loadcase (C) are 2.0. The maximum node displacement GRFs of Loadcase (D) in directions *x*, *y*, *z* are 2.0, 2.3 and 2.0, respectively, while those of Loadcase (C) are 1.8, 2.0, 1.6, respectively. Hence,

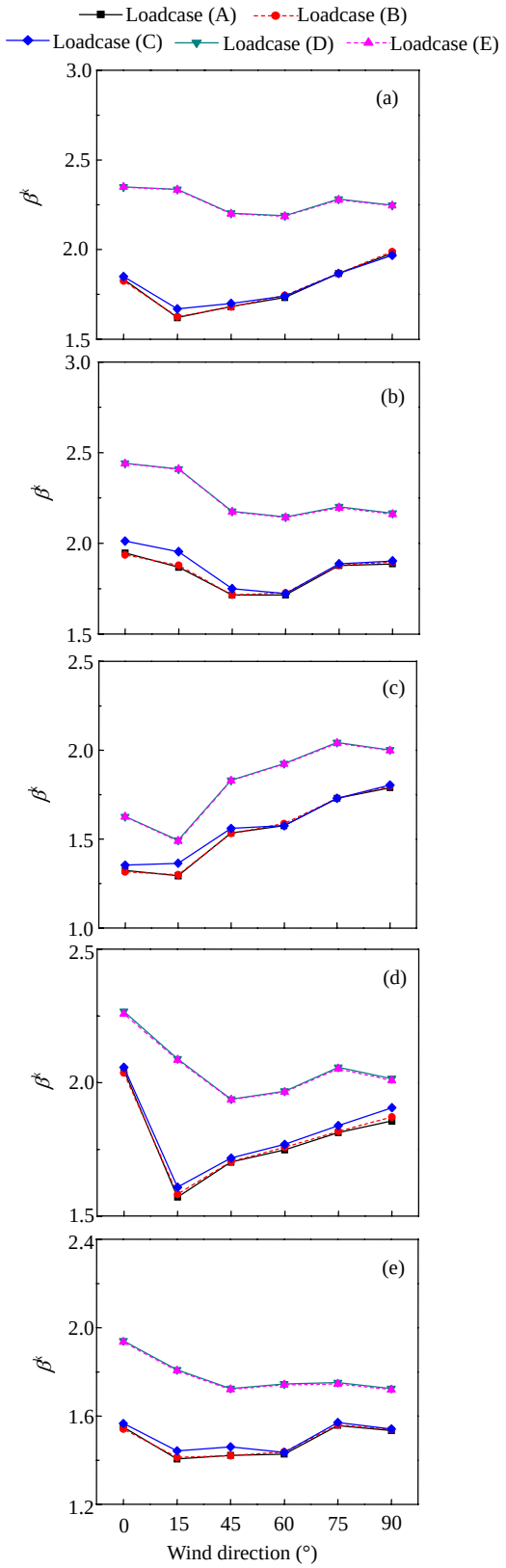

Fig.5 GRFs of (a) cable; (b) membrane; (c) nodal displacement *x*; (d) nodal displacement *y* and (e) nodal displacement *z*

the amplifications of the GRFs for Loadcase (D) are nearly 10%~25% larger than those of GRFs for Loadcase (C). The fact indicates that the correlations of the three wind load components have distinct effects on the responses of the structure. The correlations among the three wind load components need to be considered for the time-history analysis of the structure.

CONCLUSION

For a spatial 3D structure, such as a cable-membrane structure, the wind loading is a dominant factor. A model for simulating a 3D wind velocity field considering correlations of three orthogonal turbulent components is first presented in this paper. Then formulae of transforming the wind velocities into wind loads are derived in detail, also the modified wind pressure force is considered. Finally, the correlated 3D wind loads are applied to a typical spatial 3D cable-membrane structure for the wind-induced time-history response analysis. The results indicate that the GRFs obtained by the proposed correlated wind field model are 10%~25% larger than those by the traditional uncorrelated wind field model. Moreover, the modified wind pressure force has little effect on the time-history analysis. Therefore, it can be concluded that the correlations of the three wind turbulent components can not be neglected for wind-induced vibration analysis of the 3D spatial cable-membrane structure, while the modified wind pressure force can be omitted.

It should be mentioned that dynamic properties of a 3D spatial structure are very complicated, more experiments and measurements are needed to investigate the application of the proposed theory. This is an issue for future work.

References

Chen, B., Wu, Y., Shen, S.Z., 2005. Wind-induced response analysis of conical membrane structures. *Journal of Harbin Institute of Technology (New Series)*, **12**(5):481-487.

Deodatis, G., 1996. Simulation of ergodic multivariate stochastic processes. *Journal of Engineering Mechanics*, **122**(8):778-787. [doi:10.1061/(ASCE)0733-9399(1996)122:8(778)]

ESDU85020, 1985. Characteristics of Atmospheric Turbulence near the Ground. Part II: Single Point Data for Strong Winds (Neutral Atmosphere). Engineering Sciences Data Unit, London.

GB 50009-2001, 2002. Load Code for the Design of Building Structures. China Architecture and Building Press, Beijing, China (in Chinese).

Li, Y.L., Liao, H.L., Qiang, S.Z., 2004. Simplifying the simulation of stochastic wind velocity fields for long cable-stayed bridges. *Computers & Structures*, **82**(20-21):1591-1598. [doi:10.1016/j.compstruc.2004.05.007]

Luo, J.J., Han, D.J., 2008. A fast simulation method of stochastic wind field for long-span structures. *Engineering Mechanics*, **25**(3):96-101 (in Chinese).

Panofsky, H.A., Dutton, J.A., 1984. Atmospheric Turbulence. John Wiley and Sons, New York.

Shen, S.Z., 2006. Recent advances on the fundamental research of spatial structures in China. *Journal of the International Association for Shell and Spatial Structures*, **47**(151):93-100.

Shen, S.Z., Xu, C.B., Zhao, C., 2006. Design of Cable Structures (2nd Ed.). China Architecture and Building Press, Beijing (in Chinese).

Shiau, B.S., Chen, Y.B., 2002. Observation on wind turbulence characteristics and velocity spectra near the ground at the coastal region. *Journal of Wind Engineering and Industrial Aerodynamics*, **90**(12-15):1671-1681. [doi:10.1016/S0167-6105(02)00278-7]

Simiu, E., Scanlan, R.H., 1986. Wind Effects on Structures (2nd Ed.). John Wiley and Sons, New York.

Solari, G., Piccardo, G., 2001. Probabilistic 3-D turbulence modeling for gust buffeting of structures. *Probabilistic Engineering Mechanics*, **16**(1):73-86. [doi:10.1016/S0266-8920(00)00010-2]

Uematsu, Y., Isyumov, N., 1999. Wind pressures acting on low-rise buildings. *Journal of Wind Engineering and Industrial Aerodynamics*, **82**(1-3):1-25. [doi:10.1016/S0167-6105(99)00036-7]

Yang, Q.S., Sun, X.D., 1997. Horizontal and vertical wind excitations. *Journal of Harbin University of Architecture and Engineering*, **30**(6):43-50 (in Chinese).

Yang, Q.S., Shen, S.Z., 1996. Wind-resistant design of cable roof structures. *Spatial Structures*, **2**(3):23-31 (in Chinese).

Yu, S.C., Lou, W.J., Sun, B.N., 2006. Wind-induced internal pressure fluctuations of structure with single windward opening. *Journal of Zhejiang University SCIENCE A*, **7**(3):415-423. [doi:10.1631/jzus.2006.A0415]

Yu, S.C., Lou, W.J., Sun, B.N., 2008. Wind-induced internal pressure response for structure with single windward opening and background leakage. *Journal of Zhejiang University SCIENCE A*, **9**(3):313-321. [doi:10.1631/jzus.A071271]